EUROPEAN SYNCHROTRON RADIATION FACILITY

INSTALLATION EUROPEENNE DE RAYONNEMENT SYNCHROTRON

Experiment Report Form

ESRF	**Experiment title:** *Grazing incident X-ray diffraction of zeolitic benzimidazolate framework thin films for application as active coatings in solid-state chemical sensors*	**Experiment number**: *A26-2-959*
Beamline: BM26	**Date of experiment**: from: 24 January 2023 to: 27 January 2023	**Date of report**: 10 April 2023
Shifts: 9	**Local contact(s)**: dr. Martin Rosenthal	*Received at ESRF:*

Names and affiliations of applicants:

Giel Arnauts, dr. Víctor Rubio Giménez, Jennifer Theissen, Nathalie Wauteraerts

Centre for Membrane Separations, Adsorption, Catalysis, and Spectroscopy (cMACS), KU Leuven, Leuven, Belgium

Report:

Metal-organic frameworks (MOFs) are crystalline microporous coordination polymers built from metal ions or clusters connected by organic linker molecules, that offer large internal surface areas and tailorable pore interiors, qualifying them as interesting candidates for a number of applications.[1] Towards the integration of MOFs as thin films in solid-state devices, we had demonstrated a MOF chemical vapor deposition process (MOF-CVD)[2] and the potential scalability of this approach.[3]

In this work, we extend the scope of MOF-CVD to two different zeolitic imidazolate framework (ZIF) materials, ZIF-7 and ZIF-11,[4] that show particular promise for separating small gases or vapors, thanks to their narrow pore windows.[5] These materials, constructed of Zn^{2+} and benzimidazole building blocks, show different crystalline topologies and therefore functional properties. Introduction of porogen templates during synthesis allows the formation of the different crystalline phases. Figure 1 shows the unit cell of ZIF-11 as part of the RHO topology framework (a) as well as the deposition process for ZIF-11 (b), which involves the conversion of a zinc oxide precursor into MOF in presence of the linker and template vapor. During this beamtime, we wanted to investigate the stability of such films in typical device fabrication steps and their potential for post-functionalization, by monitoring their crystallinity measured with the GIWAXS setup at the BM26 beamline.

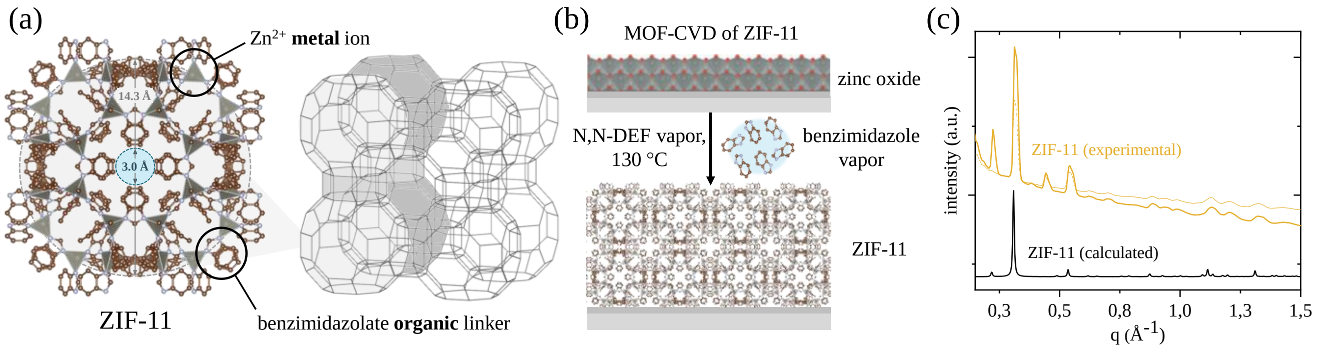

Figure 1: (a) Unit cell of ZIF-11, shown as part of RHO topology framework (b) Schematic of ZIF-11 CVD (c) X-ray diffractograms of ZIF-11 before (light orange, dashed line) and after (light orange, solid line) activation compared to calculated diffractogram (black)

First, ZIF-7 and ZIF-11 thin films were deposited under pre-optimized process conditions. After deposition, the pores were cleared from residual precursor vapor by applying a heating treatment under vacuum. The effect of this activation procedure is reflected in the diffractograms, via increased intensity of the Bragg peaks after activation (Figure 1c) and phase transformation,[6] for ZIF-11 and ZIF-7 respectively.
Previously, during another synchrotron beamline experiment, the Bragg intensities of the ZIF-11 diffraction peaks at low q (0.2-0.3 $Å^{-1}$) suffered from air scattering and the edge of the beamstop overlapping the Debye-Scherrer rings, so that the relative intensities of the diffraction peaks look skewed after integration of the total ring intensity. Installing a He flow between sample and detector allowed to minimize air parasitic scattering, to successfully compensate for the background from the beam (Figure 2a,b). The out-of-plane diffractogram recorded with our laboratory diffractometer is included in Figure 2a for comparison.

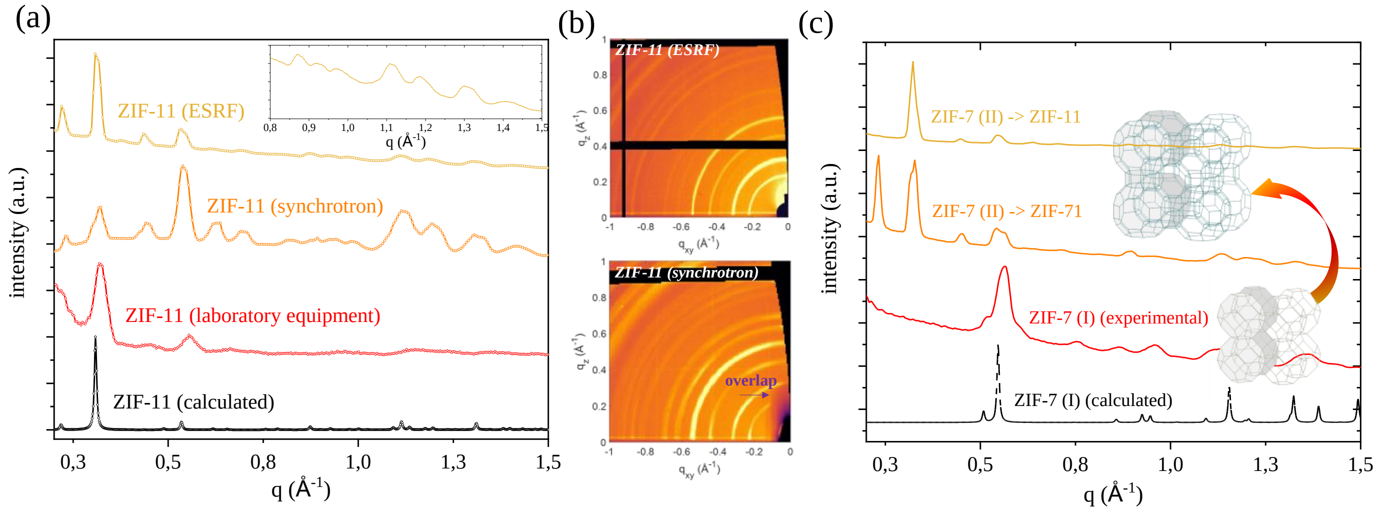

Figure 2: (a) Comparison of calculated and experimental X-ray diffractograms of ZIF-11 thin film that were recorded using different equipment (b) X-ray diffraction images of ZIF-11 thin film measured at BM26 (top) and another synchrotron source (bottom) under an incident angle σ = 0.12 (c) Vapor-phase post-functionalization of ZIF-7 (I) thin film to RHO-topology MOFs ZIF-11 and ZIF-71

Next, we looked at the robustness of ZIF-7 and ZIF-11 thin films against fabrication steps, with regard to their integration in a device layer stack. So, ZIF-7 and ZIF-11 thin films were covered with positive photoresist, exposed to a UV-lightsource for cross-linking, and then stripped from the photoresist. For both materials, a stepwise decreasing intensity of the X-ray diffraction peaks from photoresist deposition, to cross-linking and stripping was observed, which conforms to the idea that the pores are increasingly filled, as the electron density in the framework increases. However, since no additional pore activation was performed, the observed intensity decrease could also be related to material degradation. Therefore, these results will be complemented with adsorption measurements, that serve as another critical indicator of the material quality.
Finally, we explored for the first time the potential for vapor-phase post-modification of CVD ZIF thin films,[7] to enable tuning their properties towards the adsorption of a specific guest. So, the SOD ZIF-7 framework was exposed to benzimidazole and 4,5-dichloroimidazole vapor, and the template used for ZIF-11 synthesis, resulting in the transformation into RHO ZIF-11 & ZIF-71 frameworks respectively (Figure 2c). These findings disprove our previous hypothesis that vapor-phase linker-exchange is restricted to single crystal-to-single crystal transitions.[7]
In this experiment, we finetuned the grazing incident XRD characterization of CVD ZIF-7 and ZIF-11 thin films. Furthermore, we show that the crystallinity of the films is preserved after typical device fabrication steps, and that the dense ZIF-7 framework can be converted into more porous ZIFs using post-synthetic linker exchange. To complete this study, our observations will be supported by adsorption measurements, to close the gap between the observed material structure and performance of ZIF-7 and ZIF-11.

Bibliography

1. Freund, R. et al. Angewandte Chemie Int. Edit 60, 23975–24001 (2021).
2. Stassen, I. et al. Nature Mater 15, 304–310 (2016).
3. Cruz, A. J. et al. Chem. Mater. 31, 9462–9471 (2019).
4. Park, K. S. et al. Proc. Natl. Acad. Sci. U.S.A. 103, 10186–10191 (2006).
5. Jo, Y. K. et al. Nat Commun 12, 4955 (2021).
6. Zhao, P. et al. Chem. Mater. 26, 1767–1769 (2014).
7. Marreiros, J. et al. Angew. Chem. Int. Ed. 58, 18471–18475 (2019).